IEEE Access
Multidisciplinary ⋮ Rapid Review ⋮ Open Access Journal

Received December 16, 2020, accepted December 20, 2020, date of publication December 24, 2020,
date of current version January 5, 2021.

Digital Object Identifier 10.1109/ACCESS.2020.3047036

Thermal Feedback System From Robot Hand for Telepresence

YEONSEO LEE[1,2], HYEONJUNG LIM[1,3], YEUNHEE KIM[1], AND YOUNGSU CHA[1], (Senior Member, IEEE)

[1]Center for Intelligent and Interactive Robotics, Korea Institute of Science and Technology, Seoul 02792, Republic of Korea
[2]Division of Robotics, Kwangwoon University, Seoul 01897, Republic of Korea
[3]School of Mechanical Engineering, Korea University, Seoul 02841, Republic of Korea

Corresponding author: Youngsu Cha (givemong@kist.re.kr)

This work was supported by the National Research Foundation of Korea (NRF) through the Ministry of Science and ICT (MSIT), Korean Government under Grant 2020R1A2C2005252.

ABSTRACT In this study, we propose a thermal feedback system using a flexible thermal display glove (master part) and a robot hand (slave part) for telepresence. A piezoelectric sensor in the glove detects the posture of the user, which is required to operate the robot hand, while the robot hand monitors the temperature change of a grasped object and transfers the temperature feedback through thermoelectric devices mounted on the glove. Specifically, we utilize a controller to manage the thermal feedback system. Further, a series of experiments are conducted to evaluate the performance of the thermal feedback control system under heating and cooling conditions, and the responses at various desired temperatures are examined. The maximum temperature error and standard deviation under the steady-state conditions of the control system are studied. The power consumption during the response time and holding time is calculated and analyzed. Furthermore, the operation of the integrated thermal feedback system is demonstrated, and the performance of the controlled system is evaluated.

INDEX TERMS Telerobotics, thermoelectric devices, wearable sensors.

I. INTRODUCTION

As the contactless era begins, people's lifestyles and their preferred modes of communication are changing. This has led to further changes such as distance education [1], teleconference, and telecommuting [2]. Various solutions have been proposed to accommodate these changes. In particular, virtual reality (VR) [3]–[5], augmented reality (AR) [6], and teleoperation have been actively researched. Teleoperation has been widely adopted in various research fields such as telehealth [7], [8], telemaintenance [9], [10], micromanipulation [11], and disaster response [12], [13]. These researches can be theoretically analyzed [14]–[16] or focused on demonstration of system [17], [18]. To help users experience realism and immersion in a disconnected space, studies have been conducted to enhance telepresence during teleoperation [19].

For improving telepresence, various haptic systems are used: visual [20], auditory [21], and tactile stimuli [22], [23]. These tactile systems provide physical responses to humans to feel certain stimuli [5]. These systems have been developed to generate a specific tactile feedback using various methods [24], such as vibrotactile [25]–[27], pressure [28], and thermal stimuli [29], [30]. These stimuli increase the sense of realism and immersion for the users. However, many of the existing haptic devices are rigid [31] or unportable. These features make the users feel uncomfortable and limit their movement [27]. Therefore, various portable and wearable teleoperating systems have been proposed [32], [33].

To this end, we propose a thermal feedback teleoperating system using a thermal display glove with flexible thermoelectric devices (TEDs). The TEDs can generate the specified heat by the Peltier effect, which is a thermoelectric conversion effect to heating or cooling by electrical interaction between two different conductors [34]–[36]. In our previous study [37], we had demonstrated a thermal feedback glove for VR. Compared to this study, we construct a thermal feedback teleoperation system that communicates in practical environments via a robot. The posture of the hand is recognized using the thermal display glove, and the robot hand is remotely controlled. Simultaneously, the robot hand detects the temperature of the object and allows the user to feel the temperature change through the glove. Flexible TEDs are

The associate editor coordinating the review of this manuscript and approving it for publication was Zheng Chen.

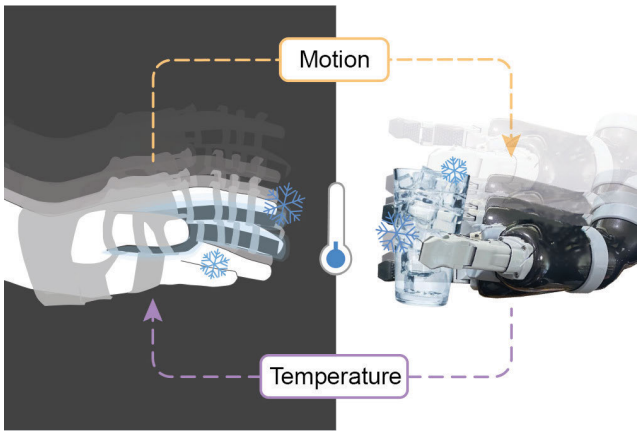

FIGURE 1. Concept of thermal feedback system using flexible thermal display glove.

mounted on the silicone glove to provide thermal feedback to the user. To control the TEDs, a thermal feedback control system is designed with a Proportional-Integral-Derivative (PID) algorithm to continuously follow the temperature changes. The performance of our thermal feedback system is evaluated by analyzing the response under various conditions of heating and cooling. Further, the maximum error in the steady-state condition and the trend of power consumed during the control process are investigated. The total thermal feedback system operation is demonstrated through the grasping of a hot or cold object. The thermal feedback of the rate of temperature change for materials with different values of thermal conductivity is also studied.

From a practical point of view, our study addresses the untapped research question about the thermal feedback from teleoperated robot. From a methodological point of view, our efforts are: (i) designing teleoperation system with thermal display glove and remote robot; (ii) conducting a systematic analysis of the role of thermal display glove for thermal feedback; and (iii) performing a thorough experimental study to demonstrate the thermal feedback system wherein the virtual objects and temperatures are systematically varied.

The remainder of this paper is organized as follows. In Section II, the system setup and operating principle of the proposed thermal feedback teleoperating system are described. In Section III, the on-off trigger control system and PID controller for tracking the temperature are described. This section also covers the details of experiments conducted for evaluation of the performance of the proposed thermal feedback system. In Section IV, the operation of the integrated thermal feedback system with the interaction of a robot hand is described. The conclusions are summarized in Section V.

II. SYSTEM DESCRIPTION

A. HARDWARE SYSTEM SETUP

The thermal feedback system comprises a thermal display glove and a robot hand, which are the master and slave parts, respectively, as shown in Fig. 2. The master system includes the silicone glove, TED control board, and interface board. The silicone glove is composed of the four TEDs, four resistance temperature detector (RTD) sensors, and three flexible piezoelectric sensors with a silicone (Ecoflex 00-30, Smooth-On, Inc.) substrate. The details of the fabrication method of the silicone glove and piezoelectric sensors have been provided in our previous paper [34]. The flexible TED (Flexible Thermoelectric Device, Tegway Co.Ltd.) is used as a thermal display to generate the specified hot or cold conditions. Four TEDs, namely, TED1 (size: 10 mm $\times$ 55 mm), TED2 (size: 10 mm $\times$ 70 mm), TED3 (size: 10 mm $\times$ 70 mm), and TED4 (size: 10 mm $\times$ 55 mm), are attached on the thumb, index finger, middle finger, and palm, respectively (see the top of Fig. 2(a)). An RTD sensor (DM-504, PT1000, size: 1 mm $\times$ 3 mm, LABFACILITY Co.,Ltd) is attached between each TED and finger using PET tape (thickness: 20 μm). In addition, a thermal pad (thickness: 2mm) is attached to the backside of each TED. Three piezoelectric sensors (thickness: 28 μm, polyvinylidene fluoride, Measurement Specialties, Inc.), namely Piezo1 (size: 5 mm $\times$ 30 mm), Piezo2 (size: 5 mm $\times$ 20 mm), and Piezo3 (size: 5 mm $\times$ 20 mm) are stuck to the silicone glove, positioned on the metacarpophalangeal joints of the thumb, index finger, and middle finger, respectively (see the middle part of Fig. 2(a)). The TED control board has a main microcontroller (ATMEGA328P-AU), Bluetooth module (F1E22, Firmtech, Inc.), and two TED drivers (VNH2SP30, 2 channels, Pololu Corp.). An analog-to-digital converter (ADC) in the microcontroller of the TED control board measures the values from the RTD sensors on the TEDs. The interface board consists of the main microcontroller (ATMEGA328P-AU) as well as the Bluetooth module (F1E22, Firmtech, Inc.), and is connected with the three piezoelectric sensors. The ADC in the microcontroller measures the piezoelectric sensor outputs through a 10 MΩ load resistor. Two 7.4 V 170 mAh lithium-ion polymer batteries are used as power sources for the interface board and TED control board, and a 5.5V DC power supply (MK3003P, MKPOWER Co.,Ltd) is used as power source for the TED driver.

The slave system includes a temperature sensing board and a robot hand (KINOVA JACO KG-3, KINOVA, Inc.). The temperature sensing board is composed of the main controller (Arduino Nano) and a Bluetooth module (FB155BC, Firmtech, Inc.), and is connected to the four RTD sensors (DM-310, PT1000, size: 2 mm $\times$ 10 mm, LABFACILITY Co.,Ltd). The sensing outputs of the RTD sensors are measured using the ADC in the temperature sensing board. These RTD sensors are attached to the three fingers and the palm of the robot hand (see the bottom part of Fig. 2(a)).

B. TOTAL SYSTEM OPERATION

Fig. 2(b) illustrates the overall system operation. The entire system communications between the master and slave parts are divided into two parts: motion control and thermal feedback control.

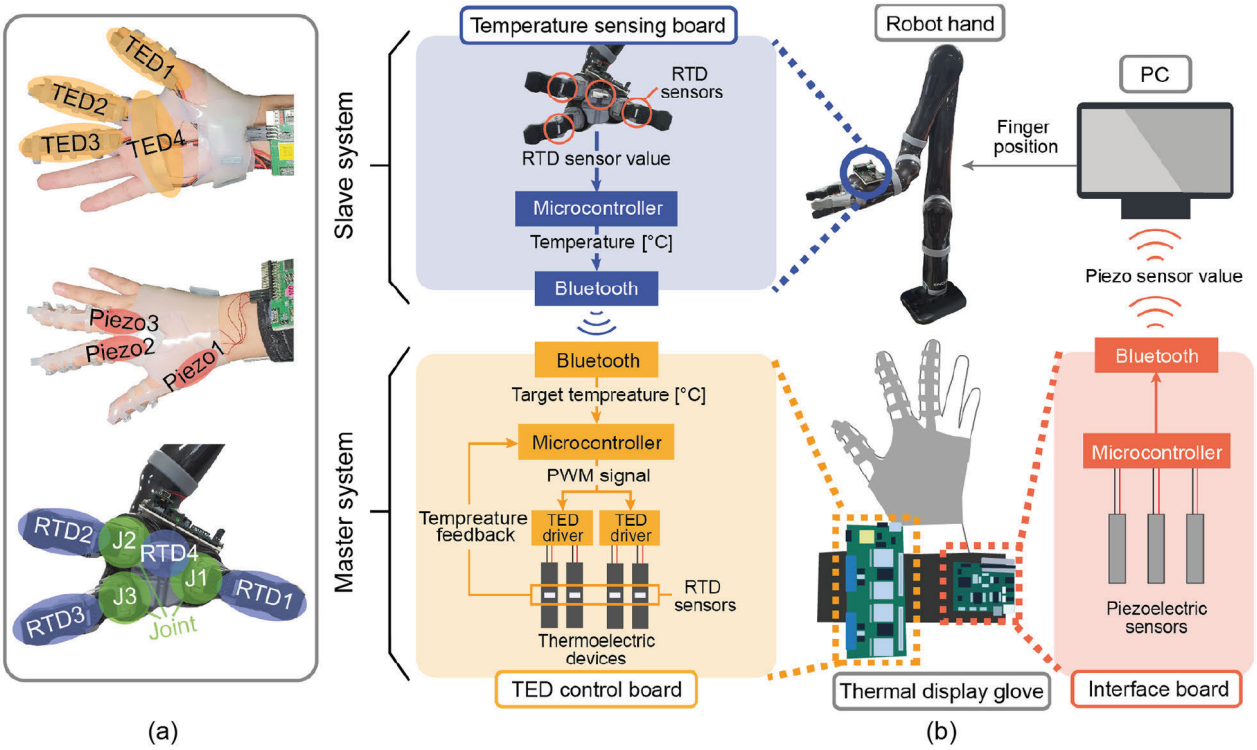

FIGURE 2. **(a) Description of the user hand with silicone glove and TED representations (top); the user hand and the piezoelectric sensor representations (middle); and the robot hand, mounted sensors, and joint representations (bottom). (b) Scheme of total thermal feedback system for telepresence with master (thermal display glove) and slave parts (robot hand).**

Motion control is implemented using the piezoelectric sensor in the master system to control the motion of the robot hand in the slave system. The piezoelectric sensors Piezo1, Piezo2, and Piezo3 correspond to the joints J1, J2, and J3 in the robot hand (Fig. 2(a)), respectively. When the user hand with the thermal display glove moves, the outputs from the piezoelectric sensors are measured by the interface board and transmitted to a PC via Bluetooth with a sampling frequency of approximately 130 Hz. We comment that sampling frequency over 100 Hz is normally used for motion recognition [38], [39]. Then, the sensor outputs are converted to the joint angles of the user [40], and they are used to operate the robot hand following the user motion.

Simultaneously, thermal feedback is conducted from the robot hand to the user with the glove. When the robot hand grasps an object during the motion of the user, the RTD sensors in the robot hand measure the temperature. Specifically, the resistance change of the RTD sensor is measured by using Wheatstone bridge circuit and amplifier. The measured resistance is converted to temperature value through the temperature-resister table in its data sheet. In the temperature sensing board, the outputs of the RTD sensors are measured and calibrated. Then, the measured temperature changes are transmitted via Bluetooth to the TED control board with a sampling frequency of approximately 80 Hz. This value is selected as maximum in the communication. This information is used to deliver thermal stimuli to the user by the TEDs in the thermal display glove. The sensor outputs of RTD1, RTD2, RTD3, and RTD4 are matched to TED1, TED2, TED3, and TED4, respectively. The half value of the temperature change in the robot hand is transferred to the user for safety. Moreover, the additional RTD sensors on the TEDs are used to control the temperature changes in the TEDs. We comment that the system can be used for long time. In this case, the temperature of the TED control board can be increased. For safety and repeatable tests, the operating time is limited.

III. THERMAL FEEDBACK

A. PID CONTROL

In order to manage the specific temperature changes of the TEDs, a PID controller is used. Specifically, the heating and cooling of the TEDs are controlled by the direction and the amount of current through Pulse Width Modulation (PWM) from the TED driver. There is the relationship between temperature change and input current in [41]. The algorithm is described in the flow chart (Fig. 3(a)) and block diagram (Fig. 3(b)) of the PID controller of our thermal feedback control system.

As shown in Fig. 3(a), an on-off trigger is set to save the power consumed during the feedback control. In addition, because humans perceive the relative difference in temperature rather than the absolute temperature [42], the relative temperature changes of the TEDs (ΔT_{TED}) should be focused on. ΔT_{TED} is following to $\Delta T_{ref} = \alpha \Delta T_{rob}$, where ΔT_{ref} and ΔT_{rob} denote the desired reference value for the TED and the

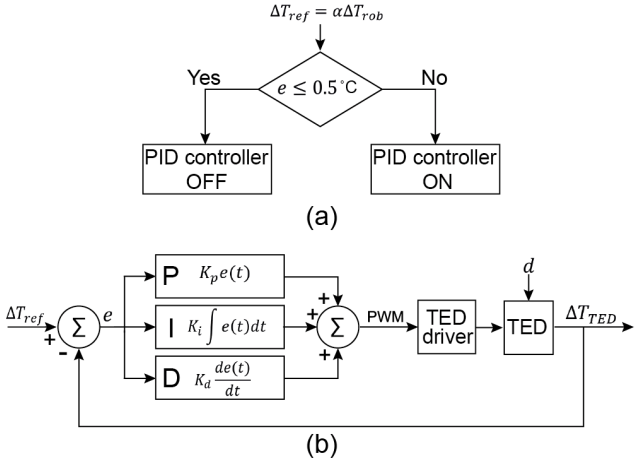

FIGURE 3. (a) Flow chart of algorithm for the total control system. (b) Block diagram of thermal feedback PID controller.

temperature change measured at the robot hand, respectively. In order to protect the users from sudden drastic thermal stimuli, the value of α is set as 0.5. During the system operation, the error $e = \Delta T_{ref} - \Delta T_{TED}$ is continuously verified. To avoid frequent power consumption of detecting subtle temperature change, the error within 0.5 °C is considered a dead zone. Therefore, the PID controller is turned on when the error exceed 0.5 °C. The control input, $u(t)$, from our PID control system is presented in Eqn. (1). Therein, the gain of proportional, integral, and differential are 120, 1, and 3, respectively.

$$u(t) = \begin{cases} 0, & \text{for } |e(t)| \leq 0.5 \\ \text{sat}(K_p e(t) + K_i \int e(t)dt + K_d \frac{de(t)}{dt}), & \text{otherwise} \end{cases} \quad (1)$$

where sat(·) denotes that control input is saturated within −255 to 255. The detailed structure of the PID controller is described in Fig. 3(b). The total control loop is 2 Hz, which is selected as maximum value in our system by preliminary tests. To communicate with TED driver, the control input, $u(t)$, from −255 to 255, is linearly mapped to duty cycle of PWM signal which has a range of 0 ∼ 100 %. The TED driver generates reversed current for cooling with a duty cycle of 0 to 50 % corresponding to a control input of −255 to 0. The TED is heated when the control input has a range of 0 ∼ 255, *i.e.*, when the range of duty cycle is from 50 to 100 %. Therefore PWM duty cycle is,

$$\text{PWM}[\%] = 50\left(\frac{u(t)}{255} + 1\right) \quad (2)$$

In other words, there is no input to TED when PWM signal has duty cycle of 50 %. At that time, ΔT_{TED} is affected by the disturbance (d) which represents the heat caused by Joule effect [43], surrounding temperature, and body temperature of the user.

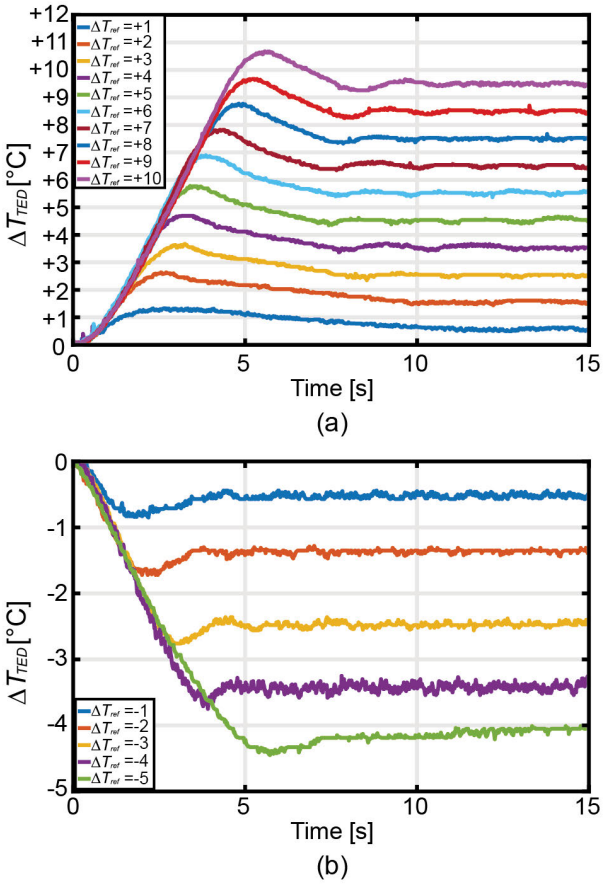

FIGURE 4. Step response of thermal feedback control system with different temperature levels between (a) +1°C to +10°C in steps of +1°C and (b) −1°C to −5°C in steps of −1°C.

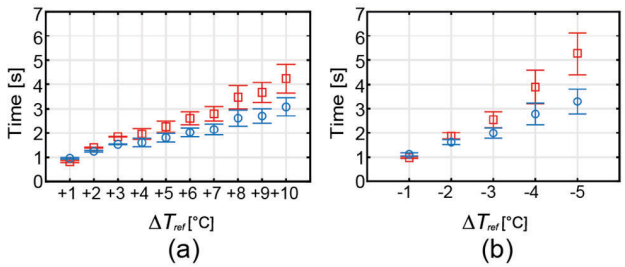

FIGURE 5. Response time (t_r) and time constant (τ) as temperature changes at (a) heating and (b) cooling. The red square and blue circle represent the average t_r and τ from five repetitive experiments. The standard deviations in the repetitive experiments are represented as error bars.

B. PERFORMANCE EVALUATION

In order to evaluate the performance of the thermal feedback control system, we establish an experimental setup. Specifically, we assume various desired temperatures and observe the response of TED2. Fig. 4(a) shows the responses for the desired temperatures in the range of +1°C to +10°C. Therein, ΔT_{ref} is given as a step input in the control system. Fig. 4(b) shows the responses for inputs in the range of −1°C to −5°C. At the same time, the RTD sensor on the TED detects the temperature change of the TED. During this

period, we measure the sensor output in serial communication with a frequency of 100 Hz. We observe that each response follows ΔT_{ref} with a steady-state error of approximately 0.5°C. It results from e_{allow} in our control system. Further, we find that the temperature changes of the TED at the various conditions have similar transient responses with a slope. We obtain the value of the slope by linear fitting using curve fitting toolbox in MATLAB. The slopes at $\Delta T_{ref} = +10$°C and -5°C are 2.3241°C/s with R-square value of 0.9979 and -1.008°C/s with R-square value of 0.9986, respectively. We comment that higher slope for the temperature change can be obtained by the increase of the input current. Although the input signal for cooling is 1.5 times larger than heating, the slew rate during the heating is more than twice the rate during cooling. The low slope during cooling may be attributed to the disturbance caused by the internal heat in the TED [43]. Thus, in our thermal feedback control, heating is easier than cooling. Therefore, these differences are assumed to be caused by the asymmetric performance of the TED between the temperature increase and decrease conditions [37], [41].

For further analysis of the responses, we obtain the values of response time (t_r) and time constant (τ). The response time is considered from the starting time to the time when the temperature reaches the control off point (0.5°C lower than the desired value). The time constant is the time when the step response reaches 63.2 % of the desired temperature. Fig. 5 shows t_r and τ along with various temperature inputs at heating (Fig. 5(a)) and cooling (Fig. 5(b)). The values are obtained from five repetitive experiments. Within, we note that t_r and τ tend to increase along with the increase of ΔT_{ref}, and their standard deviations also tend to increase. Also, the response in the heating condition is faster than that in the cooling condition at the identical magnitude of ΔT_{ref}. This shows the difference in performance between heating and cooling.

Moreover, the error ($| e_{max} |$) at the steady-state condition is shown in Fig. 6. $| e_{max} |$ represents the maximum error for the time interval (10 $\sim$ 15 s) in Fig. 4. In same time interval, $| e_{max} |$ for every experiments lies in the range of 0.5°C to 0.8°C at heating (Fig. 6(a)), and 0.5°C to 1°C at cooling (Fig. 6(b)). When ΔT_{ref} is +1°C and +10°C, the values of $| e_{max} |$ are 0.5°C and 0.74°C, respectively. In addition, when ΔT_{ref} is -1°C and -5°C, the values of $| e_{max} |$ are 0.56°C and 0.99°C, respectively. $| e_{max} |$ tends to increase with $| \Delta T_{ref} |$. Furthermore, the standard deviation for the steady-state time (σ_{steady}) is calculated. In most of the test ranges, σ_{steady} has under 0.1°C, as shown in Figs. 6(c) and (d). Thus, the thermal feedback control system is expected to maintain a stable temperature state.

Finally, we study the power consumption of the thermal feedback control system. Fig. 7 shows the power consumed by the TED (P) during t_r and holding time (t_h). Herein, holding time denotes the time for 5 seconds after t_r. P_r and P_h are the average power consumptions during the time intervals t_r and t_h, respectively. We calculate the power using

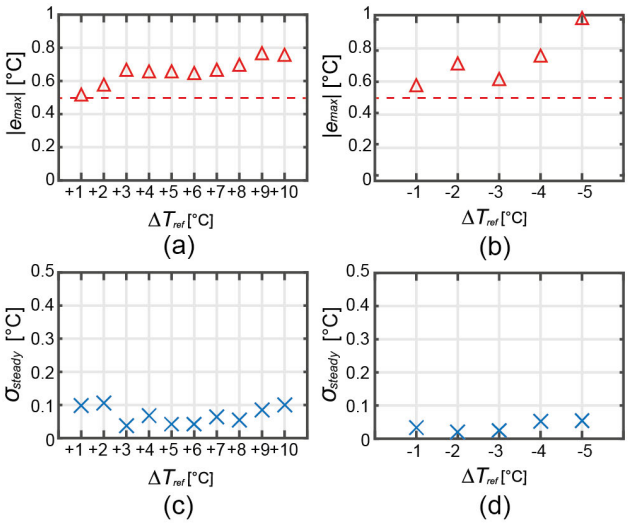

FIGURE 6. Maximum error of thermal feedback control system for steady-state time at (a) heating and (b) cooling. Standard deviation of thermal feedback control system for steady-state time at (c) heating and (d) cooling. The red triangle, blue cross, and red dotted line represent $| e_{max} |$, σ_{steady}, and e_{allow}, respectively.

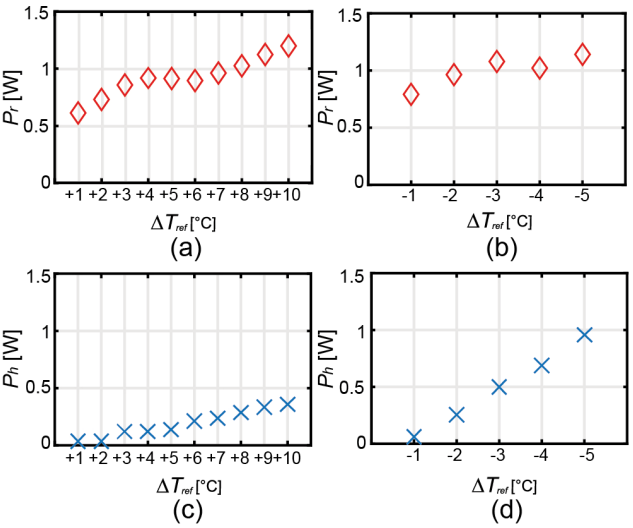

FIGURE 7. Average power consumed by the TED for response time (P_r) at (a) heating and (b) cooling. Average power for holding time (P_h) at (c) heating and (d) cooling. The red diamond and blue cross represent P_r and P_h, respectively.

the formula $P = \frac{1}{T}\int_0^T \frac{V(t)^2}{R} dt$, where P, T, V, t, and R are the average power, total time interval, voltage applied to the TED, time variable, and resistance of the TED, respectively. In order to measure the voltage applied to the TED, we utilize a data acquisition board (DAQ NI-9239, National Instrument Corp.) with a sampling frequency of 5 kHz using Labview 2017. The resistance of the TED is 1.1051 Ω, which is measured at the initial time using a multimeter (DMM7510 71/2-Digit Graphical Sampling Multimeter, Tektronix, Inc.). Figs. 7(a) and (b) present P_r in the heating and cooling conditions, respectively. While the power for +3°C consumes under 1 W, P_r about 1 W is needed for +4°C $\sim$ +8°C.

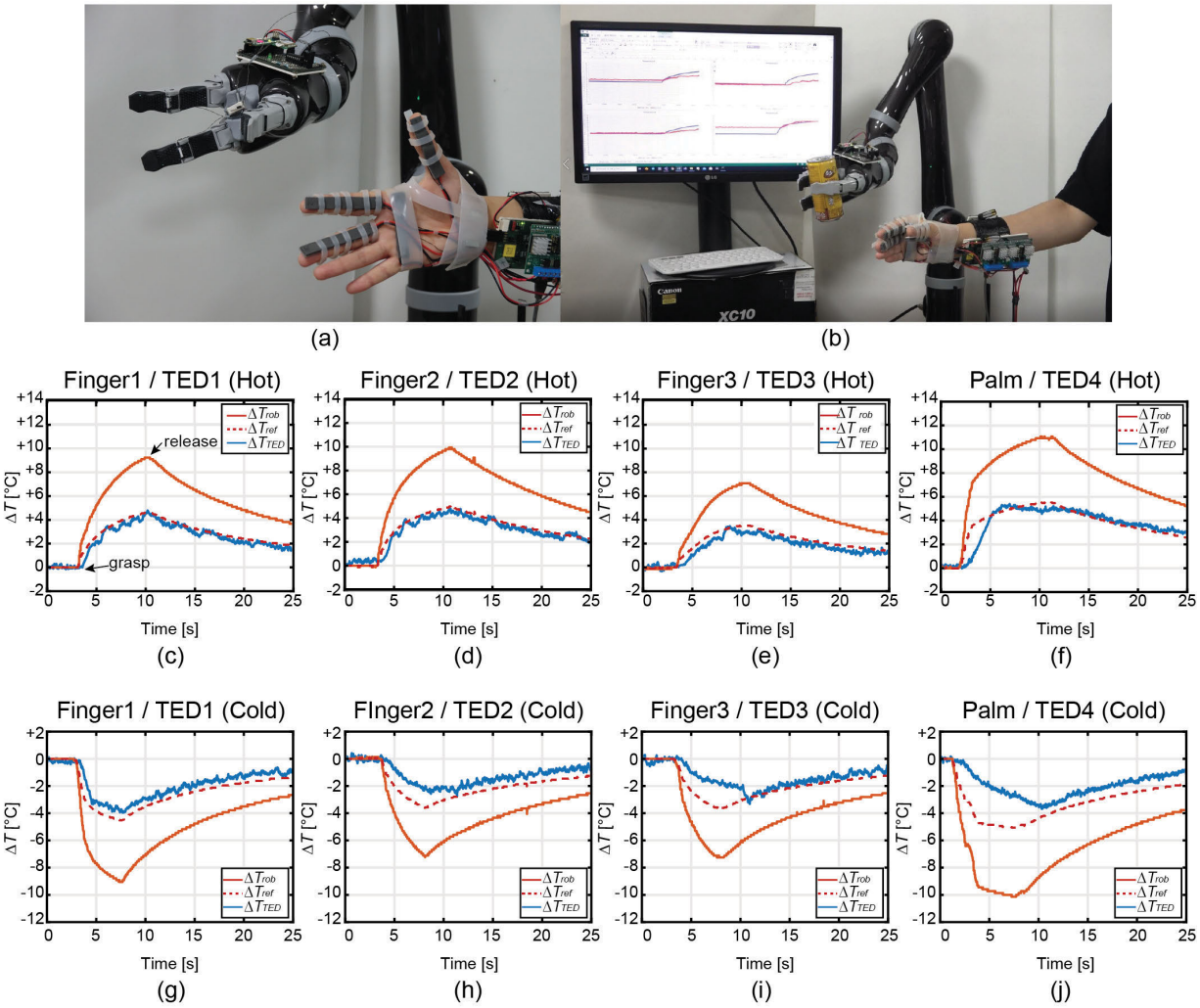

FIGURE 8. Photograph of complete thermal feedback teleoperating system with (a) initial posture and (b) grasping posture. The experimental results of (c) Finger1 (RTD1) / TED1 (Hot), (d) Finger2 (RTD2) / TED2 (Hot), (e) Finger3 (RTD3) / TED3 (Hot), and (f) Palm (RTD4) / TED4 (Hot) when the robot hand grasps a hot aluminium can and (g) Finger1 / TED1 (Cold), (h) Finger2 / TED2 (Cold), (i) Finger3 / TED3 (Cold), and (j) Palm / TED4 (Cold) when the robot hand grasps a cold aluminium can. The red solid line, red dotted line, and blue solid line represent ΔT_{rob}, ΔT_{ref}, and ΔT_{TED}, respectively.

Moreover, +9°C and +10°C need 1.1244 W and 1.1998 W, respectively. In cooling case, higher power is required. In particular, the power at −5°C is comparable to that at +10°C. Figs. 7(c) and (d) describe P_h for the heating and cooling, respectively. P_h increases with $|\ \Delta T_{ref}\ |$, because the TED is subjected to more thermal and mechanical stresses at a large temperature difference [41]. In the heating condition, when ΔT_{ref} is +1°C and +5°C, the values of P_h are 0.0003 W and 0.1080 W, respectively. In the cooling condition, when ΔT_{ref} is −1°C and −5°C, the values of P_h are 0.0605 W and 0.9583 W, respectively. This indicates that more power is consumed to maintain the temperature at the cooling than heating.

IV. SYSTEM RESULTS

A. SYSTEM OPERATION

We demonstrate the operation of the thermal feedback control system at hot and cold temperature. Fig. 8(a) shows the photograph of the robot hand and the user's hand equipped with the thermal display glove. This posture shows the initial position of the robot hand and user's hand. When the user grasps with the hand as shown in Fig. 8(b), the robot hand also follows the motion and grasps the object. Simultaneously, the temperature of the object is measured with ΔT_{rob} at the robot hand and the TEDs generate the temperature of ΔT_{ref} on the glove. In this period, we measure ΔT_{rob} and ΔT_{ref} when the robot hand grasps and releases the aluminium can in hot and cold conditions. Figs. 8(c) - (f) present the temperature change of the robot hand and TEDs in hot condition. ΔT_{TED} at TED1,2, and 3 follows the trend of ΔT_{ref}. However, TED4 at the palm shows a discrepancy at the initial dramatic rising time. This result may be attributed to the limited performance of our controller, as mentioned in Section III-B. In addition, Figs. 8(g) - (j) show the temperature changes in the cold condition. The discrepancy between ΔT_{TED} and ΔT_{ref} at the cold condition is larger than that at the hot condition.

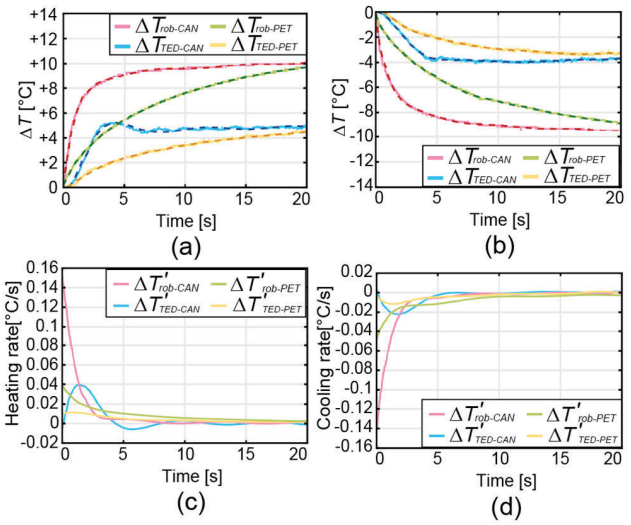

FIGURE 9. Experimental results with an aluminium can and PET bottle in (a) hot state and (b) cold state. The pink, blue, green, and yellow colors represent $\Delta T_{rob-CAN}$, $\Delta T_{TED-CAN}$, $\Delta T_{rob-PET}$, and $\Delta T_{TED-PET}$, respectively. The solid and dotted lines are experimental results and fitted values, respectively. The rate of temperature change during (c) heating and (d) cooling obtained from the fitted results.

This is because of the difference in the performance at the heating and cooling in our system as described in Section III-B.

B. TEMPERATURE CHANGE RATE

We investigate the difference in temperature transfer rate between two materials in our thermal feedback teleoperating system. The experiment is conducted with an aluminium can and a PET bottle, which have thermal conductivity of 237 W/m·K [44] and 0.15 $\sim$ 0.24 W/m·K [45], respectively. Fig. 9 shows the temperature change in the hot and cold states of the aluminium can and PET bottle in the RTD1 finger of the robot hand and TED1. The difference between the objects and room temperature is approximately $\pm$ 10°C. Simultaneously, we verify that $\Delta T_{TED-CAN}$ and $\Delta T_{TED-PET}$ approach the half values of $\Delta T_{rob-CAN}$ and $\Delta T_{rob-PET}$, respectively. We find that the slope of temperature change is different for each material. For further analysis, we calculate the rate of temperature change. Specifically, we fit $\Delta T_{rob-CAN}$, $\Delta T_{TED-CAN}$, $\Delta T_{rob-PET}$, and $\Delta T_{TED-PET}$ with a 9^{th}-order polynomial with the curve fitting tool in MATLAB (Figs. 9(a) and (b)). Then, we differentiate the fitted results of the temperature. Figs. 9(c) and (d) illustrate the rate of temperature change in the hot state and cold state, respectively. We observe that the thermal glove shows a larger rate of temperature change with the aluminium can than with the PET bottle. Therefore, we confirm that our thermal feedback system can demonstrate the rate of temperature change according to thermal conductivity.

V. CONCLUSION

In this paper, we proposed the thermal feedback teleoperating system with a thermal display glove. We composed the double-unilateral control system with the thermal display glove and a robot hand. The thermal display glove was composed of all flexible components. The communications between the master and slave parts were implemented by synchronizing the piezoelectric sensors and thermal stimuli. In order to adapt the thermal feedback in glove, we used flexible TEDs and constructed a thermal feedback control system with PID algorithm. The performance of the temperature controller was tested various levels of temperature at heating and cooling. Moreover, we investigated the power consumption with the TED at heating and cooling conditions. We found that more power was consumed to change and maintain the temperature at the cooling than heating. Finally, we demonstrated the total thermal feedback teleoperation system by that the robot hand grasped a hot or cold object. Moreover, we tested feasibility of obtaining the rate of temperature change as thermal conductivity of the objects in our system. The main contributions of this study are as follows: 1) suggesting the thermal feedback teleoperation system with a flexible thermal display glove and robot hand, 2) testing the performance of the proposed thermal feedback under various conditions, and 3) demonstrating the novel thermal feedback as the rate of temperature change. Future work should investigate theoretically the effect of the thermal conductivity by various objects. It can be used for demonstrate thermal feedback from various objects in virtual reality [37].

ACKNOWLEDGMENT

The authors would like to thank Chaewon Oh for her help with drawing schematic.

REFERENCES

[1] W. H. Snow and J. K. Coker, "Distance counselor education: Past, present, future," *Prof. Counselor*, vol. 10, no. 1, pp. 40–56, Mar. 2020.
[2] R. Yawson, "Strategic flexibility analysis of hrd research and practice post COVID-19 pandemic," *Hum. Resource Develop. Int.*, vol. 23, no. 4, pp. 406–417, 2020.
[3] S. Cai, P. Ke, T. Narumi, and K. Zhu, "ThermAirGlove: A pneumatic glove for thermal perception and material identification in virtual reality," in *Proc. IEEE Conf. Virtual Reality 3D User Interfaces (VR)*, Mar. 2020, pp. 248–257.
[4] J. Steuer, "Defining virtual reality: Dimensions determining telepresence," *J. Commun.*, vol. 42, no. 4, pp. 73–93, Dec. 1992.
[5] M. Kim, C. Jeon, and J. Kim, "A study on immersion and presence of a portable hand haptic system for immersive virtual reality," *Sensors*, vol. 17, no. 5, p. 1141, May 2017.
[6] C. Nuzzi, S. Ghidini, R. Pagani, S. Pasinetti, G. Coffetti, and G. Sansoni, "Hands-free: A robot augmented reality teleoperation system," in *Proc. 17th Int. Conf. Ubiquitous Robots (UR)*, Jun. 2020, pp. 617–624.
[7] J. E. Hollander and B. G. Carr, "Virtually perfect? Telemedicine for COVID-19," *New England J. Med.*, vol. 382, no. 18, pp. 1679–1681, Apr. 2020.
[8] R. E. Schoonmaker and C. G. L. Cao, "Vibrotactile force feedback system for minimally invasive surgical procedures," in *Proc. IEEE Int. Conf. Syst., Man Cybern.*, vol. 3, Oct. 2006, pp. 2464–2469.
[9] D. Aschenbrenner, M. Fritscher, F. Sittner, M. Krauß, and K. Schilling, "Teleoperation of an industrial robot in an active production line," *IFAC-PapersOnLine*, vol. 48, no. 10, pp. 159–164, 2015.
[10] E. Garcia, H. Guyennet, J. C. Lapayre, and N. Zerhouni, "A new industrial cooperative tele-maintenance platform," *Comput. Ind. Eng.*, vol. 46, no. 4, pp. 851–864, Jul. 2004.
[11] J. Cecil, M. B. R. Kumar, Y. Lu, and V. Basallali, "A review of micro-devices assembly techniques and technology," *Int. J. Adv. Manuf. Technol.*, vol. 83, nos. 9–12, pp. 1569–1581, 2016.

[12] J. C. Jurmain, A. J. Blancero, M. J. A. Geiling, P. A. Bennett, P. C. Jones, P. J. Berkley, P. M. Vollenweider, P. M. Minsky, P. J. C. BowersoxMD, and M. J. M. Rosen, "HazBot: Development of a telemanipulator robot with haptics for emergency response," *Amer. J. Disaster Med.*, vol. 3, no. 2, pp. 87–97, Mar. 2008.

[13] R. R. Murphy, K. L. Dreger, S. Newsome, J. Rodocker, E. Steimle, T. Kimura, K. Makabe, F. Matsuno, S. Tadokoro, and K. Kon, "Use of remotely operated marine vehicles at Minamisanriku and Rikuzentakata Japan for disaster recovery," in *Proc. IEEE Int. Symp. Saf., Secur., Rescue Robot.*, Nov. 2011, pp. 19–25.

[14] Z. Chen, F. Huang, W. Sun, and W. Song, "An improved wave-variable based four-channel control design in bilateral teleoperation system for time-delay compensation," *IEEE Access*, vol. 6, pp. 12848–12857, 2018.

[15] C. P. Vo, X. D. To, and K. K. Ahn, "A novel force sensorless reflecting control for bilateral haptic teleoperation system," *IEEE Access*, vol. 8, pp. 96515–96527, 2020.

[16] D. Chen, X. Zhou, J. Li, J. He, X. Yu, L. Zhang, and W. Qi, "A muscle teleoperation system of a robotic rollator based on bilateral shared control," *IEEE Access*, vol. 8, pp. 151160–151170, 2020.

[17] R. Luz, J. Corujeira, L. Grisoni, F. Giraud, J. L. Silva, and R. Ventura, "On the use of haptic tablets for UGV teleoperation in unstructured environments: System design and evaluation," *IEEE Access*, vol. 7, pp. 95431–95442, 2019.

[18] R. Saltaren, A. R. Barroso, and O. Yakrangi, "Robotics for seabed teleoperation: Part-1—Conception and practical implementation of a hybrid seabed robot," *IEEE Access*, vol. 6, pp. 60559–60569, 2018.

[19] A. Hosseini and M. Lienkamp, "Enhancing telepresence during the teleoperation of road vehicles using HMD-based mixed reality," in *Proc. IEEE Intell. Vehicles Symp. (IV)*, Jun. 2016, pp. 1366–1373.

[20] H. Yamada and T. Muto, "Development of a hydraulic tele-operated construction robot using virtual reality: New master-slave control method and an evaluation of a visual feedback system," *Int. J. Fluid Power*, vol. 4, no. 2, pp. 35–42, Jan. 2003.

[21] S. Hörner, S. Labus, C. Leimpeters, C. Nappert, A. Ruschkowski, B. Talhi, B. Wirth, and M. Raab, "Navigation via echolocation-like auditory feedback," *Outlook*, 2011.

[22] Y. Shen, Y. Liu, and K. Li, "Haptic tactile feedback in teleoperation of a multifingered robot hand," in *Proc. 3rd World Congr. Intell. Control Autom.*, vol. 1, Jun./Jul. 2000, pp. 85–90.

[23] Y. Shen, W. Lo, K. Li, and Y. Liu, "Haptic feedback in teleoperation of multifingered robot hands," *Intell. Autom. Soft Comput.*, vol. 9, no. 3, pp. 143–154, Jan. 2003.

[24] V. Yem and H. Kajimoto, "Wearable tactile device using mechanical and electrical stimulation for fingertip interaction with virtual world," in *Proc. IEEE Virtual Reality (VR)*, Mar. 2017, pp. 99–104.

[25] T. Debus, T. Becker, P. Dupont, T.-J. Jang, and R. D. Howe, "Multichannel vibrotactile display for sensory substitution during teleoperation," *Proc. SPIE*, vol. 4570, pp. 42–49, Feb. 2002.

[26] D. A. Kontarinis and R. D. Howe, "A multiparameter tactile display system for teleoperation," *IFAC Proc. Volumes*, vol. 28, no. 15, pp. 83–88, Jun. 1995.

[27] J. Bimbo, C. Pacchierotti, M. Aggravi, N. Tsagarakis, and D. Prattichizzo, "Teleoperation in cluttered environments using wearable haptic feedback," in *Proc. IEEE/RSJ Int. Conf. Intell. Robots Syst. (IROS)*, Sep. 2017, pp. 3401–3408.

[28] I. Sarakoglou, N. Garcia-Hernandez, N. G. Tsagarakis, and D. G. Caldwell, "A high performance tactile feedback display and its integration in teleoperation," *IEEE Trans. Haptics*, vol. 5, no. 3, pp. 252–263, 3rd Quart., 2012.

[29] A. Drif, J. Citerin, and A. Kheddar, "Thermal bilateral coupling in teleoperators," in *Proc. IEEE/RSJ Int. Conf. Intell. Robots Syst.*, Aug. 2005, pp. 1301–1306.

[30] S. Gallo, L. Santos-Carreras, G. Rognini, M. Hara, A. Yamamoto, and T. Higuchi, "Towards multimodal haptics for teleoperation: Design of a tactile thermal display," in *Proc. 12th IEEE Int. Workshop Adv. Motion Control (AMC)*, Mar. 2012, pp. 1–5.

[31] Y. Masuda, D. Nagahama, H. Itahara, T. Tani, W. S. Seo, and K. Koumoto, "Thermoelectric performance of Bi- and na-substituted $Ca_3Co_4O_9$ improved through ceramic texturing," *J. Mater. Chem.*, vol. 13, no. 5, pp. 1094–1099, Apr. 2003.

[32] B. Fang, D. Guo, F. Sun, H. Liu, and Y. Wu, "A robotic hand-arm teleoperation system using human arm/hand with a novel data glove," in *Proc. IEEE Int. Conf. Robot. Biomimetics (ROBIO)*, Dec. 2015, pp. 2483–2488.

[33] B. Fang, F. Sun, H. Liu, D. Guo, W. Chen, and G. Yao, "Robotic teleoperation systems using a wearable multimodal fusion device," *Int. J. Adv. Robot. Syst.*, vol. 14, no. 4, 2017, Art. no. 1729881417717057.

[34] S. H. Kim, Y. Kwon, K. Kim, and Y. Cha, "Estimation of hand motion from piezoelectric soft sensor using deep recurrent network," *Appl. Sci.*, vol. 10, no. 6, p. 2194, Mar. 2020.

[35] X. Qiu and J. Yuan, "Temperature control for PCR thermocyclers based on Peltier-effect thermoelectric," in *Proc. IEEE Eng. Med. Biol. 27th Annu. Conf.*, Jan. 2006, pp. 7509–7512.

[36] F. J. DiSalvo, "Thermoelectric cooling and power generation," *Science*, vol. 285, no. 5428, pp. 703–706, Jul. 1999.

[37] S.-W. Kim, S. H. Kim, C. S. Kim, K. Yi, J.-S. Kim, B. J. Cho, and Y. Cha, "Thermal display glove for interacting with virtual reality," *Sci. Rep.*, vol. 10, no. 1, pp. 1–12, Dec. 2020.

[38] H. Jeon, S. L. Kim, S. Kim, and D. Lee, "Fast wearable sensor–based foot–ground contact phase classification using a convolutional neural network with sliding-window label overlapping," *Sensors*, vol. 20, no. 17, p. 4996, Sep. 2020.

[39] J. Zhang, S. Liu, Y. Zhang, and R. Zhu, "A method to extract motion velocities of limb and trunk in human locomotion," *IEEE Access*, vol. 8, pp. 120553–120561, 2020.

[40] K. Song, S. H. Kim, S. Jin, S. Kim, S. Lee, J.-S. Kim, J.-M. Park, and Y. Cha, "Pneumatic actuator and flexible piezoelectric sensor for soft virtual reality glove system," *Sci. Rep.*, vol. 9, no. 1, pp. 1–8, Dec. 2019.

[41] S. J. Kim, H. E. Lee, H. Choi, Y. Kim, J. H. We, J. S. Shin, K. J. Lee, and B. J. Cho, "High-performance flexible thermoelectric power generator using laser multiscanning lift-off process," *ACS Nano*, vol. 10, no. 12, pp. 10851–10857, Dec. 2016.

[42] G. Wilson, M. Halvey, S. A. Brewster, and S. A. Hughes, "Some like it hot: Thermal feedback for mobile devices," in *Proc. Annu. Conf. Hum. Factors Comput. Syst. (CHI)*, 2011, pp. 2555–2564.

[43] M. Ishii, Y. Hibino, F. Hanawa, H. Nakagome, and K. Kato, "Packaging and environmental stability of thermally controlled arrayed-waveguide grating multiplexer module with thermoelectric device," *J. Lightw. Technol.*, vol. 16, no. 2, pp. 258–264, Feb. 1998.

[44] K. Chu, C. Jia, X. Liang, H. Chen, H. Guo, F. Yin, and X. Qu, "Experimental and modeling study of the thermal conductivity of SiCp/Al composites with bimodal size distribution," *J. Mater. Sci.*, vol. 44, no. 16, pp. 4370–4378, Aug. 2009.

[45] H. Malekpour, K.-H. Chang, J.-C. Chen, C.-Y. Lu, D. L. Nika, K. S. Novoselov, and A. A. Balandin, "Thermal conductivity of graphene laminate," *Nano Lett.*, vol. 14, no. 9, pp. 5155–5161, Sep. 2014.

YEONSEO LEE is currently pursuing the B.S. degree with the Division of Robotics, Kwangwoon University, Seoul, South Korea. She was a Research Trainee with the Center for Intelligent and Interactive Robotics, Korea Institute of Science and Technology (KIST), Seoul. Her current research interests include soft mechatronics, wearable robotics, and teleoperation systems.

HYEONJUNG LIM is currently pursuing the M.S. degree in mechanical engineering from Korea University, Seoul, South Korea. She is also a Research Trainee with the Center for Intelligent and Interactive Robotics, Korea Institute of Science and Technology (KIST), Seoul. Her current research interests include soft actuator, wearable robotics, and smart materials and structures.

YEUNHEE KIM received the M.S. degree in mechanical engineering from Korea University, Seoul, South Korea. She is currently an Intern Researcher with the Center for Intelligent and Interactive Robotics, Korea Institute of Science and Technology (KIST), Seoul. Her current research interests include soft mechatronics, robotics, energy harvesting, and smart materials and structures.

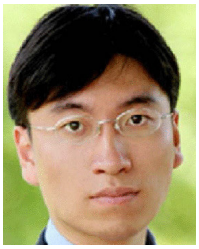

YOUNGSU CHA (Senior Member, IEEE) received the B.S. degree in electrical engineering from Korea University, Seoul, South Korea, in 2004, the M.S. degree in electrical engineering from the Korea Advanced Institute of Science and Technology (KAIST), Daejeon, South Korea, in 2007, and the Ph.D. degree in mechanical engineering from New York University, New York, NY, USA, in 2015. He is currently a Principal Research Scientist with the Center for Intelligent and Interactive Robotics, Korea Institute of Science and Technology (KIST), Seoul. His current research interests include smart materials and structures, multiphysics modeling, flexible sensors and actuators, energy harvesting, and robotics.